JOURNAL OF GEOPHYSICAL RESEARCH, VOL. 112, C09011, doi:10.1029/2006JC004024, 2007

Click Here for Full Article

On the extreme statistics of long-crested deep water waves: Theory and experiments

Nobuhito Mori,[1] Miguel Onorato,[2] Peter A. E. M. Janssen,[3] Alfred R. Osborne,[2] and Marina Serio[2]

Received 21 November 2006; revised 14 March 2007; accepted 7 June 2007; published 15 September 2007.

[1] Quasi-resonant four-wave interactions may influence the statistical properties of deep water long-crested surface gravity waves. As a consequence, the wave height exceedance probability can substantially deviate from the expected distribution obtained by assuming that waves are linear. Here the occurrence probability of extreme events recently derived by N. Mori and P. Janssen (2006) is compared with wave tank data, where strong departures from Gaussian behavior are observed. Experimental wave height, maximum wave height distribution, and probability of occurrence of freak waves are compared with theoretical expectations. The theory well predicts extreme waves in nonlinear wavefields.

Citation: Mori, N., M. Onorato, P. A. E. M. Janssen, A. R. Osborne, and M. Serio (2007), On the extreme statistics of long-crested deep water waves: Theory and experiments, *J. Geophys. Res.*, *112*, C09011, doi:10.1029/2006JC004024.

1. Introduction

[2] In the last decades a lot of effort in the oceanographic community has been dedicated to the study of extreme events in the ocean. In years 2004 and 2005, three conferences/workshop, Rogue Waves 2004 held in Brest, France [*Olagnon and Prevosto*, 2004], Rogue Waves in Hawaii [*Muller and Henderson*, 2005], and ICMS Workshop on Rogue Waves in Edinburgh, UK, and sessions in large conferences, such as European Geosciences Union [*Pelinovsky and Kharif*, 2006], were completely devoted to the study of extreme waves. The state on the art on the subject can be found in the proceedings of the conferences. Nowadays, it is accepted that at least four mechanisms are responsible for the formation of extreme waves. The first one is just a linear superposition of waves; in this case the probability distribution for wave height in the limit of the narrow-band approximation obeys a Rayleigh distribution [*Longuet-Higgins*, 1952]; corrections due to finite spectral bandwidth have been obtained [*Næss*, 1985; *Boccotti*, 1989; *Tayfun*, 1981]. Wave crest statistics can be achieved by using the second-order theory developed by *Longuet-Higgins* [1963]. In the narrow-band approximation, the probability distribution for wave crests has been given by *Tayfun* [1980] (for finite bandwidth, see *Fedele and Arena* [2005]). The second mechanism is the interaction of waves with currents: linear theory can explain the formation of extreme waves using ray theory. The statistical properties of the surface elevation as a function of the properties of the currents are so far unknown. The third mechanism, the one that will be mainly discussed here, concerns the generation of extreme events as a result of the modulational instability, i.e., a four wave quasi-resonant interaction process [e.g., *Yasuda et al.*, 1992; *Yasuda and Mori*, 1994; *Onorato et al.*, 2001; *Janssen*, 2003]. This mechanism becomes relevant for long-crested waves; in the case of waves with directional spreading it is still not clear what is the role of the modulational instability and consequent formation of extreme events. Numerical results in freely decaying case [*Onorato et al.*, 2002; *Socquet-Juglard et al.*, 2005] have shown that the addition of a directional spreading decreases the probability of formation of extreme waves, leading to wave crests distributed according to the Tayfun distribution [*Socquet-Juglard et al.*, 2005]. The fourth mechanism is related to crossing sea states, i.e., two sea systems, for example a swell and a wind sea, with different directions that coexists in some region of the ocean. In deep water, modulational instability in crossing seas can also play a role [*Onorato et al.*, 2006]: the presence of a second sea system can trigger some instability in the first sea state that, if alone, would be stable. The evidence of freak wave generation in the real ocean analyzing were reported by analyzing field data of the North Sea [*Stansell et al.*, 2003; *Guedes Soares et al.*, 2003], the Sea of Japan [*Yasuda and Mori*, 1997; *Yasuda et al.*, 1997], and the Gulf of Mexico [*Guedes Soares et al.*, 2004].

[3] An ultimate goal in all these studies of extreme waves is indeed the determination of the shape of the exceedance probability function. Once the analytical form is found for all sea state conditions (for example as a function of the wave spectrum), the probability of finding a wave that exceeds a certain height can be directly estimated. For example, if one considers the Rayleigh distribution as a reference distribution for wave heights then, the probability of appearance of a wave larger than twice the significant wave height is about 1/2980. The one difficulty of extreme

[1] Graduate School of Engineering, Osaka City University, Osaka, Japan.
[2] Dipartmento di Fisica Generale, Università di Torino, Turin, Italy.
[3] European Centre for Medium-Range Weather Forecasts, Reading, UK.

Copyright 2007 by the American Geophysical Union.
0148-0227/07/2006JC004024$09.00

study is the verification of the theory. The statistical theories are evaluated under the assumptions of stationarity. However, the real sea state changes both spatially and temporally. Therefore the statistical theories are difficult to verify [i.e., *Mori et al.*, 2002]. In addition, freak wave prediction requires the prediction of the maximum wave height distribution. Thus the verification of the wave height distribution is insufficient and the discussion of the maximum wave height distribution is needed to complete the verification of freak wave prediction [*Stansell et al.*, 2003; *Mori and Janssen*, 2006].

[4] Recently some experimental work has been conducted in a very large wave tank facility in Norway [*Onorato et al.*, 2004, 2005b, 2006]. One of the aims of these experiments was to determine the shape of the distribution function for wave heights for random, long-crested waves in deep water. The experiments have highlighted that there are some conditions for which the exceedance probability derived from the Rayleigh distribution underestimates by almost an order of magnitude the probability of measuring a wave larger than twice the significant wave height. This discrepancy could not be explained in terms of the second-order theory and has been associated to the modulational instability phenomenon that takes place in random waves. The presence of extreme events is accompanied by a strong departure of the surface elevation kurtosis from the expected Gaussian value. The relationship between the kurtosis and the extreme wave events has been discussed during the last decade (e.g., for the laboratory data [*Mori et al.*, 1997], for the numerical results [*Yasuda and Mori*, 1994], and for the field data [*Guedes Soares et al.*, 2004]). This is of course not a surprise because the kurtosis is the fourth-order moment of the probability density function; therefore it is a measure of the relevance of the tails in a distribution. *Mori and Janssen* [2006; see also *Tayfun and Lo*, 1990; *Mori and Yasuda*, 2002] discuss the formal relation between the kurtosis and the exceedance probability for wave height. The kurtosis enters in the distribution function as a correction to the Rayleigh distribution: when the kurtosis tends to three, the expected Gaussian values, then the distribution function tends to the Rayleigh distribution. In this context, the changes in the kurtosis can be evaluated once the evolution of the wave spectrum is known [see *Janssen*, 2003]. *Mori and Janssen* [2006] derived the wave height exceedance probability as a function of the considered number of waves.

[5] The conditions under which large deviations have been observed experimentally are characterized by large steepness and narrow band spectra. This experimental result was consistent with previous analytical and numerical studies in weakly nonlinear wave models [*Onorato et al.*, 2001; *Janssen*, 2003] in which the ratio between the steepness, a measure of the nonlinearity and the spectral bandwidth, a measure of the dispersion, has been identified as an important parameter for determining the probability of finding a large wave. After this ratio between nonlinearity and dispersion was named the Benjamin-Feir-Index (BFI), its relation to the kurtosis was given by *Janssen* [2003] in the limit of large times and for a narrow banded spectra. The final result is that the kurtosis depends on the square of the BFI. The role of the skewness in the wave height distribution is less important with respect to kurtosis. The skewness comes usually as a result of second-order corrections (bound modes) and is weakly affected by the dynamics of free waves [*Onorato et al.*, 2005a].

[6] A different approach, also based on the dynamics of cubic nonlinearity, has been used by *Fedele and Tayfun* [2006] for finding the exceedance probability for wave height. The approach is based on an optimization problem, requiring that at a specific space and time, the Fourier phases are all equal, with the constraints that the conservation laws of the Zakharov equation are satisfied. *Fedele and Tayfun* [2006] derived an analytical form for the exceedance probability; nevertheless, it is still not clear if this distribution function is the result of nonlinear corrections to a quasi-linear focusing process or that it really takes into account the modulational instability as a nonlinear self-focusing mechanism.

[7] In the present paper we will make a detailed comparison between experimental data from the Marintek wave tank facility and theory by *Mori and Janssen* [2006] of a number of statistical parameters, namely, the kurtosis evolution owing to the four wave interactions, the wave height distribution and the maximum wave height distribution. The paper is organized as follows: in section 2 a summary of the results derived by *Mori and Janssen* [2006] is given, in section 3 the experiment performed at Marintek is described, the comparison of experimental data and theory is reported in section 4. The results give the universal theory of the extreme wave generation as a consequence of four wave interactions in a unidirectional wave train.

2. Theoretical Background

2.1. Quasi-Resonant Four Wave Interactions and High-Order Moments

[8] As previously mentioned, the modulational instability is a quasi-resonant interaction process, i.e., wave numbers and frequencies satisfy the following conditions:

$$\vec{k}_1+\vec{k}_2-\vec{k}_3-\vec{k}_4=0 \quad \text{and} \quad \omega\left(\vec{k}_1\right)+\omega\left(\vec{k}_2\right)-\omega\left(\vec{k}_3\right)-\omega\left(\vec{k}_4\right)\le\epsilon^2, \tag{1}$$

here ϵ is a small parameter which corresponds to the steepness in deep water waves. More in particular, the modulational instability takes place when two wave numbers are the same $\vec{k}_1 = \vec{k}_2$ and $\vec{k}_3$ and $\vec{k}_4$ are two sidebands separated from $\vec{k}_1$ by Δk, which should be small in order to satisfy the condition (1). The standard kinetic equation that describes the evolution of the wave spectrum in time [*Hasselmann*, 1962] is formally only valid for large times, $O(\epsilon^{-4}\omega_0^{-1})$, and for exact resonances; its extension to quasi-resonant interactions has been done by *Janssen* [2003] where a kinetic equation, which should be valid also on the timescale of the modulational instability, has been derived [see also *Annekov and Shrira*, 2006]. If one then considers the evolution of higher-order moments such as the kurtosis, it turns out that the quasi-resonant interactions are responsible for deviations from Gaussian values. *Janssen* [2003] investigated the explicit relation between nonlinear interactions of free waves and the fourth-order moment of the surface elevation $\eta(\vec{x}, t)$ in deep water. The result is

$$\kappa_{40} = \frac{\langle \eta^4 \rangle}{m_0^2} - 3 = \frac{12}{g^2 m_0^2} \int \mathrm{d}\vec{k}_{1,2,3,4} T_{1,2,3,4} \sqrt{\omega_1 \omega_2 \omega_3 \omega_4} \cdot \delta_{1+2-3-4} R_r(\Delta\omega, t) N_1 N_2 N_3 \tag{2}$$

where m_0 is the variance of the surface elevation η, κ_{40} is the fourth-order cumulant of the surface elevation (equals to kurtosis minus 3), g is the acceleration of gravity, k is the wave number, ω is the angular frequency, N is the wave action spectral density, $T_{1,2,3,4}$ is the coupling coefficient in the Zakharov equation (see *Krasitskii* [1994] for its analytical form), $\delta_{1+2-3-4} = \delta(\vec{k}_1 + \vec{k}_2 - \vec{k}_3 - \vec{k}_4)$, $\mathrm{d}\vec{k}_{1,2,3,4} = \mathrm{d}\vec{k}_1\, \mathrm{d}\vec{k}_2\, \mathrm{d}\vec{k}_3\, \mathrm{d}\vec{k}_4$ and $R_r = (1 - \cos(\Delta\omega\ t))/\Delta\omega$ is the resonant function. In the limit of large times $R_r \rightarrow \mathcal{P}/\Delta\omega$, where $\Delta\omega = \omega_1 + \omega_2 - \omega_3 - \omega_4$ and $\mathcal{P}$ denotes the principle value of the integral to avoid singularity in the integral.

[9] In the narrow-band approximation, assuming that the spectrum $E(\omega)$ has a Gaussian shape:

$$E(\omega) = \frac{m_0}{\sigma_\omega \sqrt{2\pi}}\, e^{-\frac{1}{2}\nu^2}, \tag{3}$$

where $\nu = (\omega - \omega_0)/\sigma_\omega$ and σ_ω is the spectral bandwidth, the integral in (2) for large times becomes:

$$\kappa_{40} = \frac{24\epsilon^2}{\Delta^2} \mathcal{P} \int \frac{\mathrm{d}\nu_{1,2,3}}{(2\pi)^{3/2}} \frac{e^{-\frac{1}{2}\left[\nu_1^2 + \nu_2^2 + \nu_3^2\right]}}{(\nu_1 + \nu_2 - \nu_3)^2 - \nu_1^2 - \nu_2^2 + \nu_3^2}, \tag{4}$$

where $\epsilon = k_0\sqrt{m_0}$ is the steepness parameter and $\Delta = \sigma_\omega/\omega_0$ is the relative spectral bandwidth. The integral can be evaluated analytically to obtain:

$$\kappa_{40} = \frac{\pi}{\sqrt{3}} BFI^2 \tag{5}$$

where BFI is defined as by *Janssen* [2003]

$$BFI = \frac{\epsilon}{\Delta}\sqrt{2}. \tag{6}$$

Equation (5) is the simplified prediction equation of the kurtosis of the surface elevation assuming a narrow-band, unidirectional wave train, but the full description requires the evaluation of a six dimensional integral in wave number space, equation (2).

2.2. Wave Height and Maximum Wave Height Distributions

[10] In order to include nonlinear effects in the wave height distribution function giving possible deviations from the Rayleigh statistics, the standard approach is to use the Edgeworth series developed at the beginning of the last century [e.g., *Edgeworth*, 1907]. The theory for wave height is described by *Tayfun and Lo* [1990], *Mori and Yasuda* [2002], and *Mori and Janssen* [2006]. The resulting distribution has been named the Modified Edgeworth Rayleigh (MER) distribution. The MER wave height and exceedance wave height distribution are given by *Mori and Janssen* [2006]:

$$p(H)dH = \frac{1}{4} H e^{-\frac{1}{8}H^2} [1 + \kappa_{40} A_H(H)] dH, \tag{7}$$

$$P_H(H) = e^{-\frac{1}{8}H^2} [1 + \kappa_{40} B_H(H)], \tag{8}$$

where H is the wave height normalized by $\eta_{rms} = \sqrt{m_0}$, κ_{40} is defined in equation (4) and $A_H(H)$ and $B_H(H)$ are polynomials defined as

$$A_H(H) = \frac{1}{384}\left(H^4 - 32H^2 + 128\right), \tag{9}$$

$$B_H(H) = \frac{1}{384} H^2 \left(H^2 - 16\right). \tag{10}$$

Note that these distributions describe the deviation from linear statistics under the hypothesis of a narrow-band, weakly nonlinear wave train. Second-order contributions, which are important for the distribution of wave crests, can be included by using a Tayfun-like approach [*Tayfun*, 1980; see also *Tayfun*, 2006].

[11] The probability distribution function, p_m, and the exceedance probability, P_m, of the maximum wave height can also be given as a function of the fourth cumulant of the surface elevation κ_{40} and the number of waves N recorded in the wave train,

$$p_m(H_{\max}) = \frac{N}{4} H_{\max}\, \mathrm{e}^{-\frac{H_{\max}^2}{8}} [1 + \kappa_{40} A_H(H_{\max})] \times \exp\left\{-N \mathrm{e}^{-\frac{H_{\max}^2}{8}} [1 + \kappa_{40} B_H(H_{\max})]\right\}, \tag{11}$$

$$P_m(H_{\max}) = 1 - \exp\left\{-N \mathrm{e}^{-\frac{H_{\max}^2}{8}} [1 + \kappa_{40} B_H(H_{\max})]\right\}, \tag{12}$$

where $H_{\max}$ is the maximum wave height normalized by η_{rms}. *Mori and Janssen*'s [2006] comparison of the theoretical wave height distribution with field data showed qualitative agreement. For $\kappa_{40} = 0$, results are identical to the ones following from the Rayleigh distribution.

[12] Note that simpler looking expressions for the wave height and maximum wave height distribution may be obtained by normalizing with the significant wave height $H_s = 4\sqrt{m_0}$. We record these expressions for completeness. Hence normalizing with the significant wave height, equations (7)–(12) become

$$p^*(H^*)dH^* = 4H^* e^{-2H^{*2}} [1 + \kappa_{40} A_H{}^*(H^*)] dH^*, \tag{13}$$

$$P_H{}^*(H^*) = e^{-2H^{*2}} \left[1 + \kappa_{40} B_H^*(H^*)\right], \tag{14}$$

$$A_H^*(H^*) = \frac{1}{3}\left(2H^{*4} - 4H^{*2} + 1\right), \tag{15}$$

$$B_H{}^*(H^*) = \frac{2}{3} H^{*2}\left(H^{*2} - 1\right). \tag{16}$$

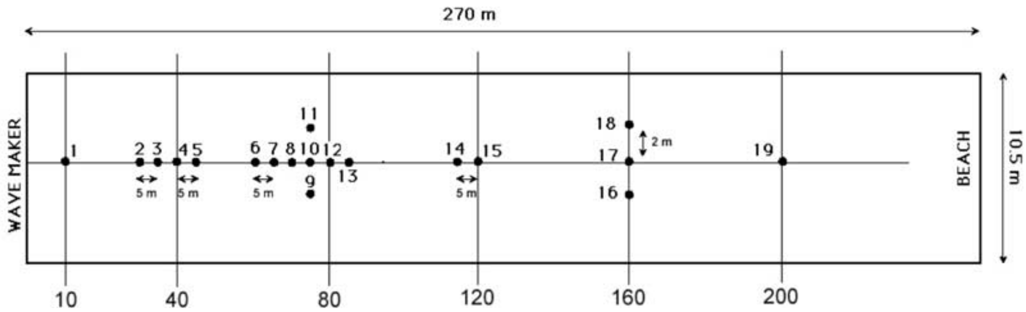

Figure 1. Sketch of the wave tank facility at Marintek and location of wave probes.

while the maximum wave height distribution and the exceedance probability becomes

$$p_m^*(H_{\max}^*) = 4NH_{\max}^* \,\mathrm{e}^{-2H_{\max}^{*2}}\left[1+\kappa_{40}A_H^*(H_{\max}^*)\right] \times \exp\left\{-N\mathrm{e}^{-2H_{\max}^{*2}}\left[1+\kappa_{40}B_H^*(H_{\max}^*)\right]\right\}, \tag{17}$$

$$P_m^*(H_{\max}^*) = 1-\exp\left\{-N\mathrm{e}^{-2H_{\max}^{*2}}\left[1+\kappa_{40}B_H^*(H_{\max}^*)\right]\right\}. \tag{18}$$

where $H_{\max}^*$ is the maximum wave height normalized by H_s.

[13] If one defines a freak wave as a wave whose height $H_{freak} \geq 2H_s$, we obtain from equation (12) or (18) the following simple formula to predict the occurrence probability of a freak wave as function of N and κ_{40},

$$P_{freak} = 1-\exp[-\beta N(1+8\kappa_{40})] \tag{19}$$

where $\beta = \mathrm{e}^{-8}$ is constant. The term $8\kappa_{40}$ is the nonlinear correction to linear theory for the maximum wave height distribution. Thus the nonlinear correction to the maximum wave height depends on κ_{40}.

[14] To summarize the above discussion, we can state that the quasi-resonant four wave interactions introduce deviations from linear expectations of the statistics of surface elevation; in particular, for weakly nonlinear, narrow-banded and long-crested wave trains, the kurtosis evolves according to equation (2). In the narrow-band approximation, the kurtosis is related to the BFI; the tail of wave height distribution depends on the kurtosis/BFI and increases as the kurtosis increases. Finally, the maximum wave height distribution depends on both the number of waves in the wave train (record length) and the kurtosis; see equation (11).

3. Experimental Data

[15] The experiment was carried out in the long-wave flume at Marintek; experimental details and some data analysis are given by *Onorato et al.* [2006]. The length of the tank is 270 m and its width is 10.5 m; the depth is 10 meters for the first 85 meters and 5 meters for the rest of the flume. For the wavelengths considered in the experiments, the deep water conditions apply through the tank. A horizontally double-hinged flap type wave maker located at one end of the tank was used to generate the waves. A sloping beach is located at the far end of the tank opposite the wave maker used. The wave surface elevation was measured simultaneously by 19 probes placed at different locations along the flume. The sampling frequency for each probe was 40 Hz. The capacitance wave gages were used for the surface displacement measurements. A view of the flume with the location of the probes is shown in Figure 1. JONSWAP random wave signals where generated at the wave maker as sums of independent harmonic components, by means of the inverse Fast Fourier Transform of complex random Fourier amplitudes. These were prepared according to the "random phase approach" by using random Fourier amplitudes as well as random phases. This implies that because of the central limit theorem, κ_{40} should ideally be equal to zero and μ_4 equal to 3. In the original experiment, three different JONSWAP spectra with different values of BFI have been investigated. Here we will consider only the most interesting case, i.e., the most nonlinear case, which corresponds to the largest BFI; this corresponds to a JONSWAP spectrum with $\gamma = 6$ and significant wave height of 16 cm, initially. As mentioned in the previous section, the maximum wave height depends on the number of waves in the wave train in both linear and nonlinear theory as shown in equation (11). Hence the large number of waves is fundamental for the convergence both of the tail of the PDF of wave height and the maximum wave height. Therefore five different realizations with different sets of random phases have been performed. The duration of each realization was 32 min. The total number of wave heights (counting both upcrossing and down-crossing) recorded for each spectral shape at each probe was about 12800 waves. This is a sufficient number of waves to check the sensitivity of the maximum wave height distribution on the number of waves. In our analysis we have removed the first 200 s of the records for each realization. This lapse of time was calculated as the approximate time needed for the wave of twice the peak frequency to reach the last probe.

4. Comparison of the Laboratory Data and Theory

4.1. Skewness and Kurtosis of Surface Elevation

[16] In Figure 2 the skewness and kurtosis of the surface elevation for the experimental data along the channel are shown. As can be noticed, both skewness and kurtosis deviate substantially from the Gaussian expected values. Traditionally, departures from Gaussian statistics have been attributed to the presence of bound waves; these waves do not obey the linear dispersion relation and are the result of random combination of Stokes like waves. The theory, up to

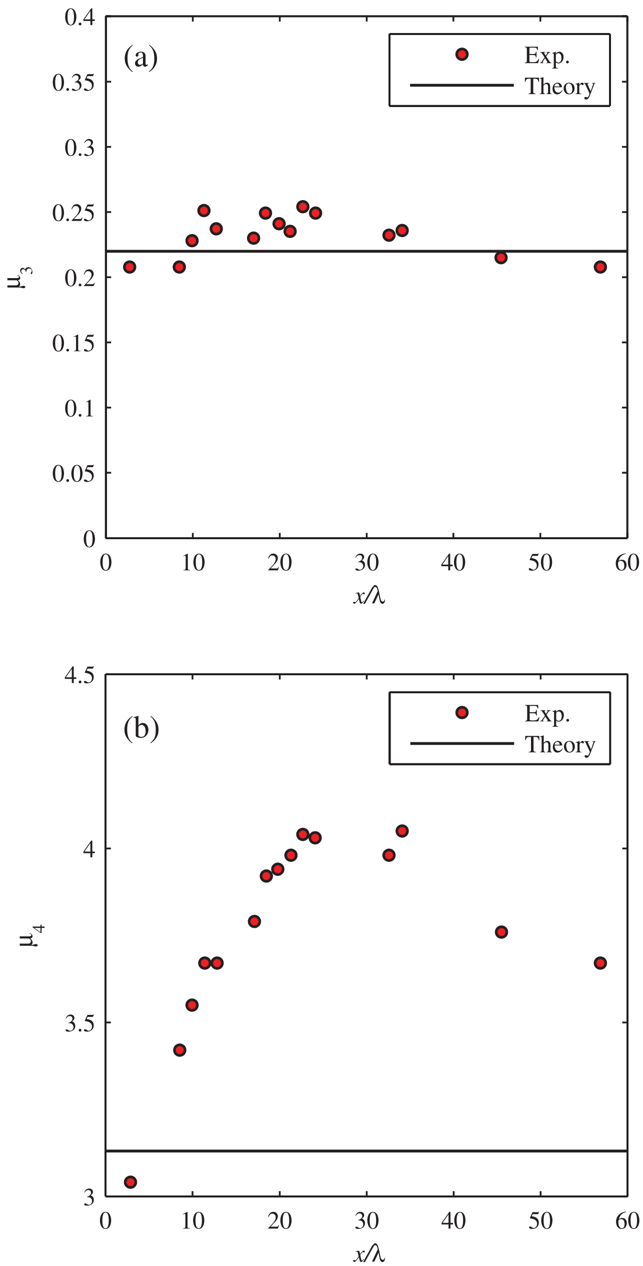

Figure 2. (a) Skewness and (b) kurtosis of the experimental data along the tank as a function of the distance from the wave maker. λ corresponds to a characteristic wavelength corresponding to the peak frequency period 1.5 s of the waves at the first probe.

second order, has been developed by *Longuet-Higgins* [1963]. In order to give here a first estimation of the skewness and kurtosis, we will adopt the narrow band approximation of the second-order theory. Under this condition the skewness, μ_3^b and kurtosis μ_4^b take the following form:

$$\mu_3^b = 3k_0 m_0^{1/2} \tag{20}$$

$$\mu_4^b = 3 + 24k_0^2 m_0 \tag{21}$$

For the present data, if one takes as m_0 the one calculated from the first probe, we obtain the following results $\mu_3^b = 0.22$ and $\mu_4^b = 3.13$. In Figure 2 the horizontal lines correspond to the expected value from second-order narrow band theory. According to (20)–(21), a simple relation between skewness and kurtosis exists: $\mu_4^b = 3 + \frac{8}{3}\mu_3^{b2}$ [see also *Marthinsen and Winterstein*, 1992; *Mori and Janssen*, 2006]; this quadratic relation, with our experimental data is shown in Figure 3. The empirical relation by *Guedes Soares et al.* [2003] is also shown in Figure 3. As can be seen there is no agreement (except for the point that corresponds to the first probe closest to the wave generator), although both the theoretical and empirical curve show qualitatively a similar tendency. As expected most of experimental data of skewness and kurtosis are underpredicted along the tank if only second-order theory is considered. This is especially true for the kurtosis; as was mentioned before, while the kurtosis can be notably influenced by the dynamics of the free modes of four wave interactions, the skewness is only weakly affected. A much better agreement between experimental data and theory can be achieved if the dynamics of free waves is included. In Figure 4 we show a comparison of the experimental data with theory, i.e., equation (2). Even though the agreement is not impressive, the theory seems to reproduce the behavior of the experimental data in a much better way than the second-order theory.

4.2. Wave Height Distribution

[17] In this section we will compare the experimental wave height distribution with results obtained using equation (8). Hereafter, for brevity, we will refer to equation (8) as the MER (Modified Edgeworth Rayleigh) distribution. Note that the use of the MER distribution implies that the kurtosis of the surface elevation is known. This can be estimated, either by theory or directly from the experimental data; the second choice has been adopted. The comparison of the experimental exceedance probability of wave heights

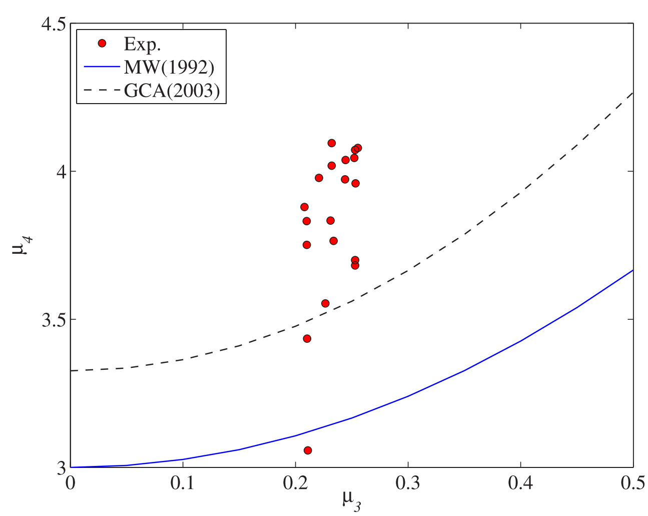

Figure 3. Relationship between skewness and kurtosis. The solid circles are the experimental data, the solid line is the second-order nonlinear theory by *Marthinsen and Winterstein* [1992], and the dashed line is the emperical fit by *Guedes Soares et al.* [2003].

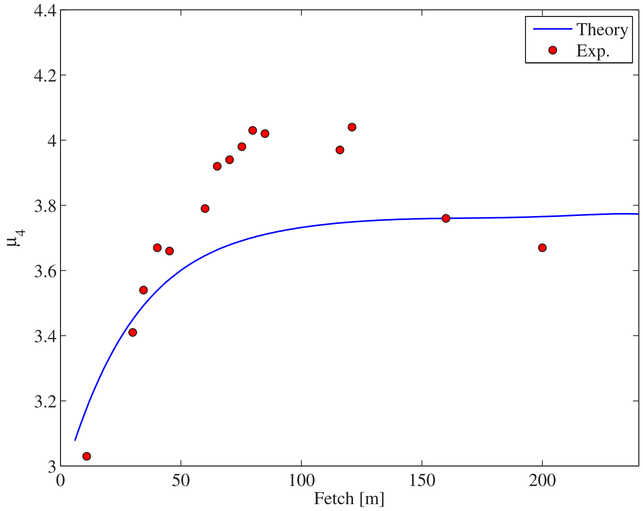

Figure 4. Kurtosis of the experimental data as a function of the distance from the wave maker compared with theoretical values obtained from quasi-resonant theory.

compared with the MER distribution is shown in Figure 5 for a number of probes located at different distances from the wave maker. Figure 5a corresponds to probe 1 in Figure 2 and is located 10 m offshore from the wave maker. Here we emphasize that waves have been generated by using the random phase approximation so that we expect that, after a few wavelengths, the surface elevation is still very close to be characterized by Gaussian distribution (the experimental value of the kurtosis is μ_4 = 3.06, i.e., almost Gaussian). As previously mentioned, as μ_4 tends to 3.0, the MER distribution tends to the Rayleigh distribution. Note that both these theoretical curves in Figure 5a overestimate the experimental results. The reason of this discrepancy may be attributed to the fact that experimental data are characterized by a spectrum that has some finite width. Similar results can be obtained by linear random simulations [i.e., *Goda*, 2000]. As waves travel along the tank, quasi resonant four wave interactions become important and, as previously described, the kurtosis of the surface elevation starts to deviate from the Gaussian value and the tail of the distribution deviates from linear expectation. This is shown in Figures 5b and 5c obtained from time series recorded respectively at about 8 and 34 wavelengths from the wave maker. Because of the aforementioned nonlinear effects, the exceedance probability obtained from the laboratory data shows some deviations for large waves from the Rayleigh distribution. The MER distribution follows this behavior; this is especially true for waves with large kurtosis as shown in Figure 5c (μ_4 = 4.10). It should be noted that the MER distribution includes only the kurtosis and does not consider the skewness, which is mainly modified by the presence of bound modes. As already denoted in the previous section, the effect of bound modes is negligible if the wave height distribution for a narrow-band wave train is considered; the second-order corrections are relevant only for the crest distribution.

[18] In Figure 6 we show the probability of occurrence of freak waves $H_{\max}/\eta_{rms} \geq 8$ for short time records, as a function of the kurtosis measured at different probes. We

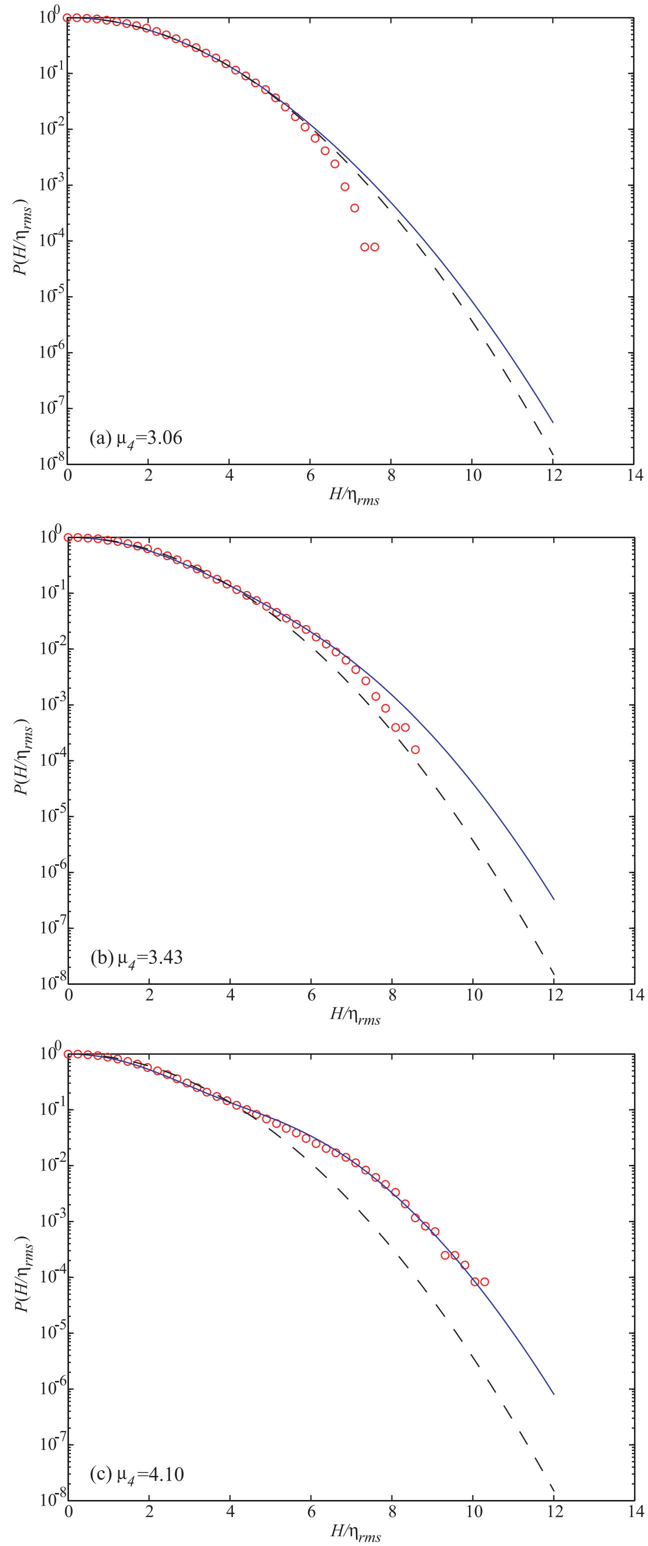

Figure 5. Comparison of exceedance wave height distribution H/η_{rms}: circles, experimental data; solid line, MER distribution/equation (8); and dashed line, Rayleigh distribution.)

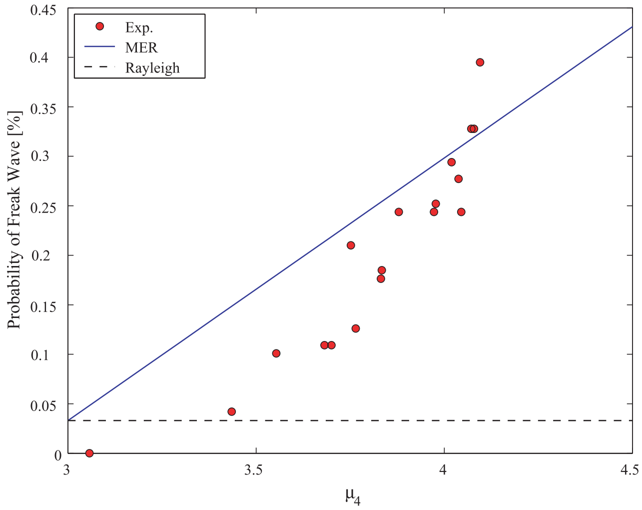

Figure 6. Occurrence probability of freak wave in the long recorded wave data N = 11900: circles, experimental data; solid line, MER distribution by equation (19); and dashed line, Rayleigh distribution.

assumed 100 number of waves for each record and counted number of freak waves. The solid circles denote the experimental data and the linear theory based on the Rayleigh distribution is represented by the dotted line, the nonlinear theory, equation (19), corresponds to the solid line. The occurrence probability of freak waves in the experimental data shows a clear dependence on the kurtosis (this effect of course is not described by the Rayleigh distribution). While the occurrence probability of freak waves estimated by the MER distribution shows a linear relation with the kurtosis, equation (19), experimental data appear to give a quadratic function of the kurtosis. This is probably because the MER includes only the lowest correction of nonlinearity and excludes high-order cumulants. Moreover, the MER seems to overestimate the occurrence probability of freak wave with respect to the experimental data for small kurtosis. This may be related to the fact that the MER distribution (as well as the Rayleigh distribution) is based on the assumption that waves are narrow banded.

4.3. Maximum Wave Height Distribution

[19] The consequences of the maximum wave height distribution (equation (11)) are in general hard to verify, not only because equation (11) depends on the number of waves considered but also because nonlinear effects are included in the distribution via the kurtosis which requires a large number of data to converge. Nevertheless, the present experimental data set seems to be suitable for such comparison (as previously described, the time series are very long). Figure 7 shows the comparison of the maximum wave height distribution from the experimental data with equation (11) for N = 150. The solid circles represent the experimental data, the maximum wave height distribution from Rayleigh theory (denoted Rayleigh $H_{\max}$ distribution hereafter) is represented by the dotted line and equation (12) (denoted by MER $H_{\max}$ distribution hereafter) corresponds to the solid line. To obtain a distribution of maximum wave height, each experimental record is divided in smaller time series containing each 150 waves; the maximum wave heights are then collected from each shorter time series. In Figure 7a the comparison between theory and experiment is shown for probe 1. The peak of the observed maximum

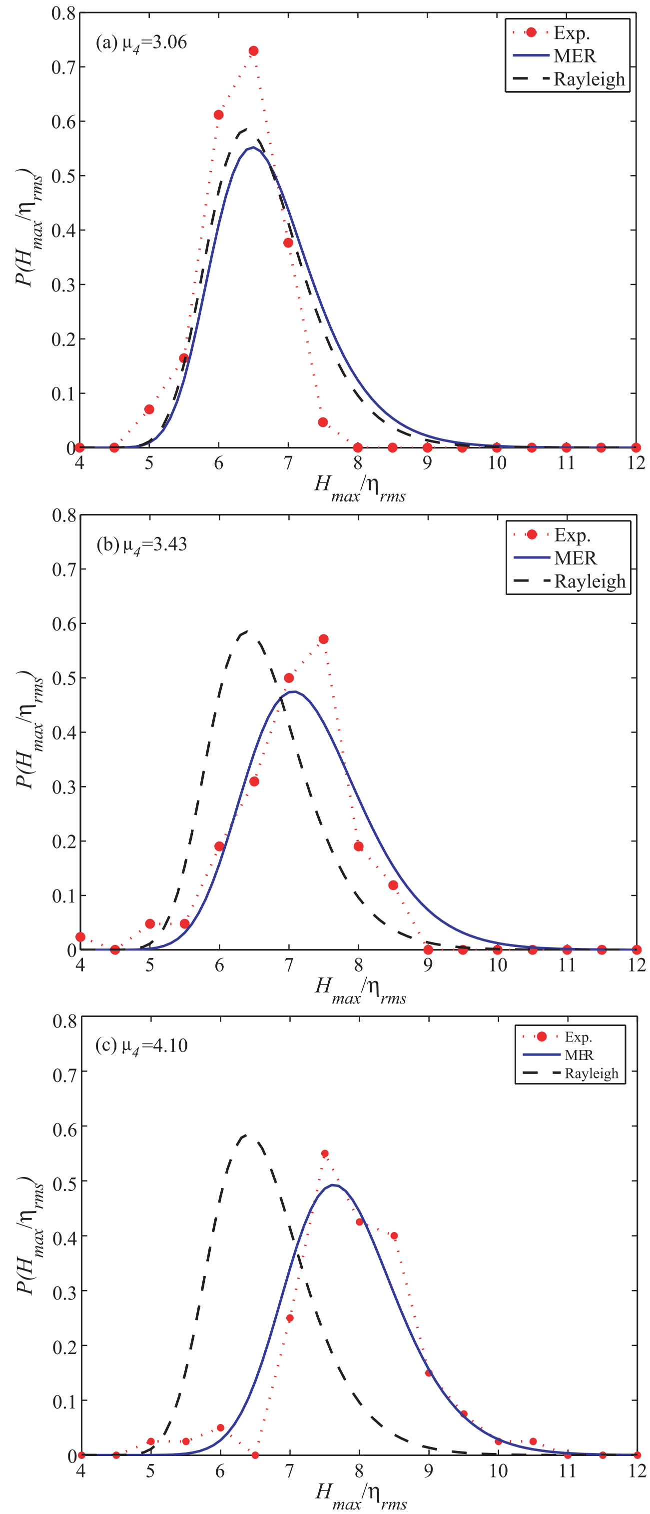

Figure 7. Comparison of maximum wave height distribution H_{max}/η_{rms} with N = 150: circles, experimental data; solid line, MER H_{max} distribution; and dashed line, Rayleigh H_{max} distribution.

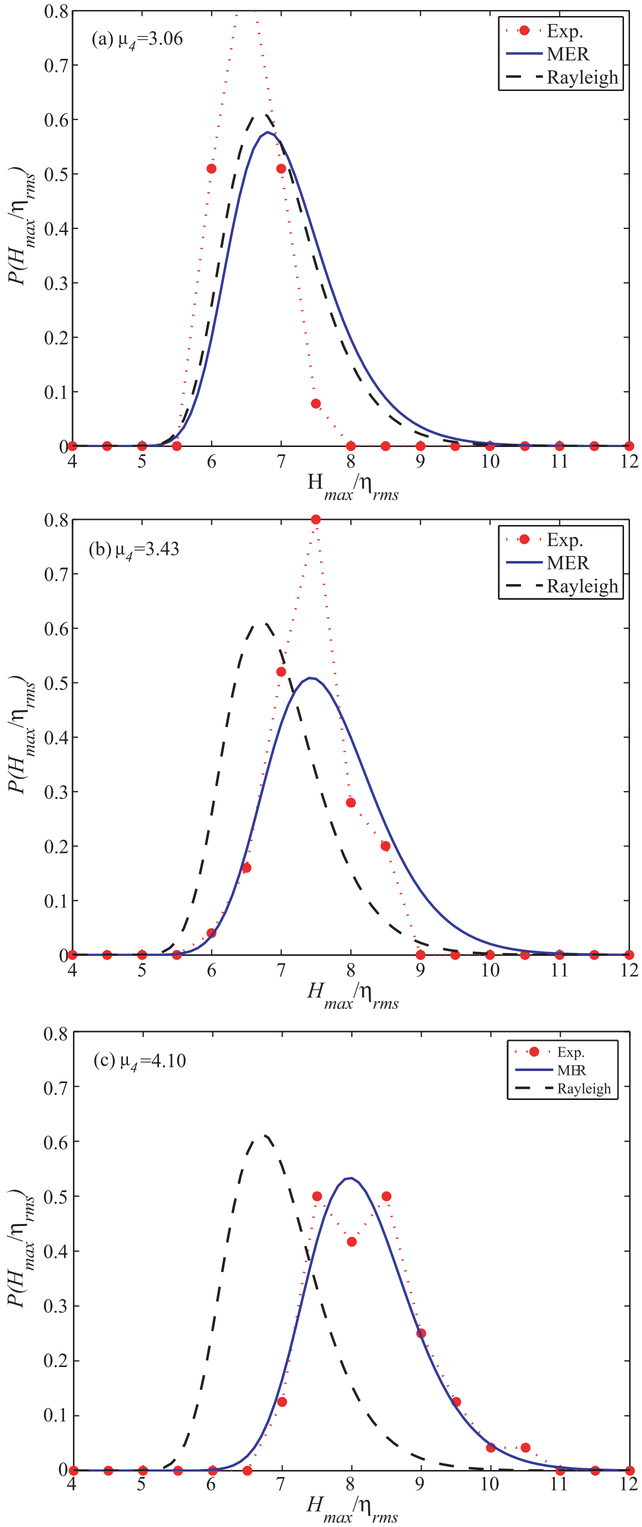

Figure 8. Comparison of maximum wave height distribution H_{max}/η_{rms} with $N = 250$: circle, experimental data; solid line, MER H_{max} distribution; and dashed line, Rayleigh H_{max} distribution.

wave height distribution is larger than the Rayleigh $H_{\max}$ distribution and the MER $H_{\max}$ distribution with $\mu_4 = 3.06$ but the observed distribution is more narrow (just as for the wave height distribution we ascribe this difference to effects of finite width of the spectrum). As waves propagate through the flume, the nonlinear dynamics result in an increase of the kurtosis, and therefore the maximum wave height distribution of the laboratory data departs from the Rayleigh distribution (Figure 7a–7c) and the peak of the observed distribution shift to larger wave heights. While the Rayleigh $H_{\max}$ distribution is independent of the kurtosis, the MER $H_{\max}$ distribution follows decently the behavior of the experimental data. Figure 8 shows similar comparisons with $N = 250$. The peak of the experimental data in the linear wave condition, Figure 8a, moves from $H/\eta_{rms} \simeq 6.2$ to $H/\eta_{rms} \simeq 6.6$ because of the change of number of waves in the wave train from 150 to 250. The MER $H_{\max}$ distribution seems to reproduce reasonably well the experimental data; for very small kurtosis, it overestimates the experimental data and for large kurtosis it slightly underestimates the data. This is consistent with what we have shown in Figure 6 where the occurrence probability of freak waves is plotted as a function of the kurtosis. Note that according to the observations and theory more than half of the number of waves in the case of $\mu_4 = 4.1$ and $N = 250$ satisfy the freak wave condition as shown in Figure 8c.

[20] Here we also discuss the general behavior of the probability density function of maximum wave height in the

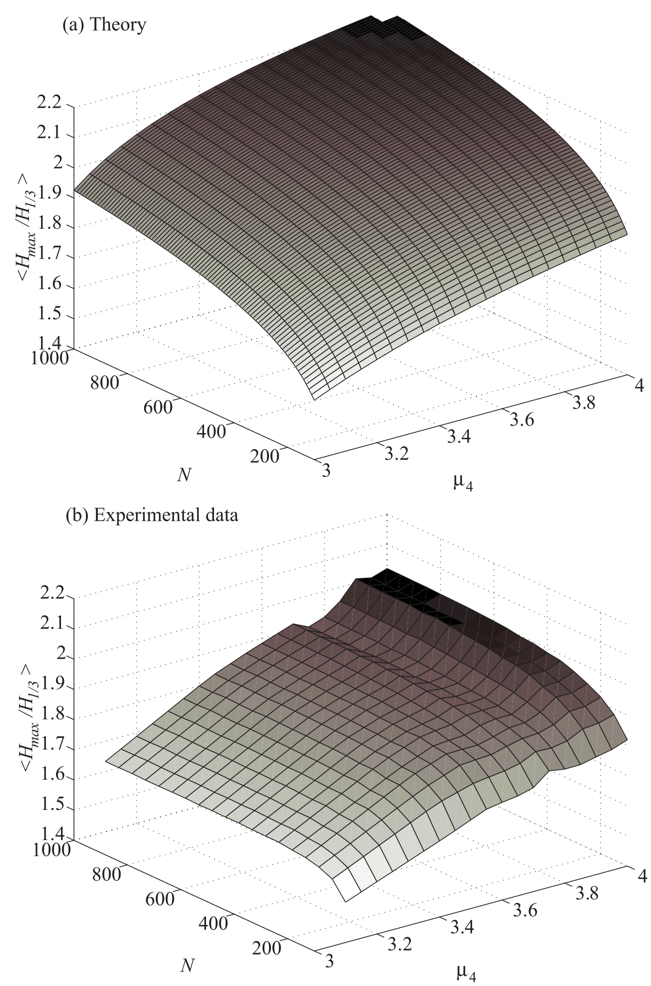

Figure 9. Comparison of expected value of $H_{\max}/H_{1/3}$, $\langle H_{\max}/H_{1/3}\rangle$.

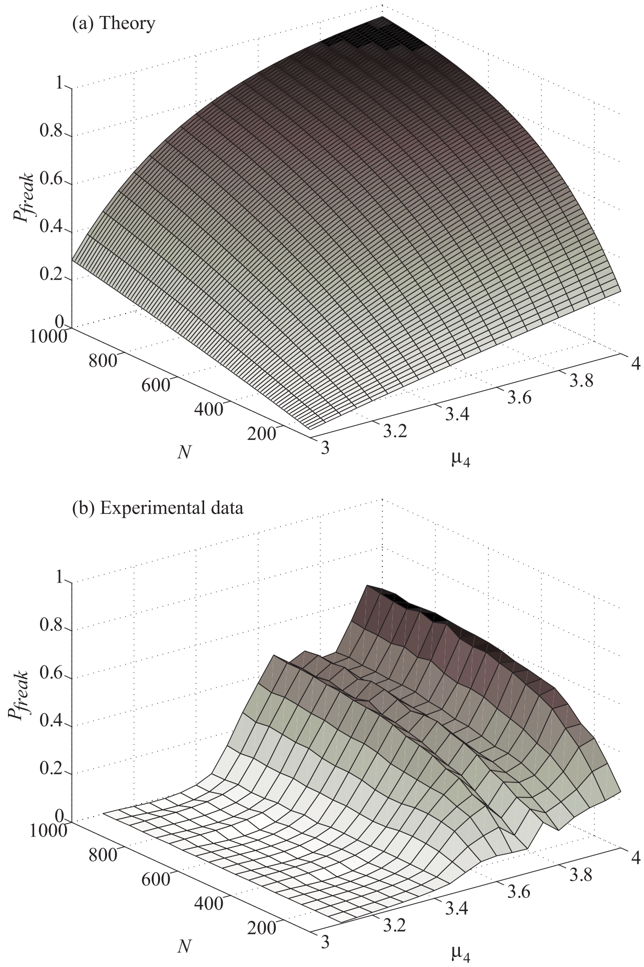

Figure 10. Comparison of occurrence probability of freak wave as a function of μ_4 and N.

nonlinear wavefield, by plotting the expected value of the maximum wave height, indicated by $\langle\rangle$, as a function of μ_4 and N, see Figure 9. In this figure we show the numerically integrated value of equation (11) and the ensemble average of the experimental data. The $\langle H_{\max}/H_{1/3}\rangle$ according to the Rayleigh theory corresponds to Figure 9 with $\mu_4 = 3$. The dependence of $\langle H_{\max}/H_{1/3}\rangle$ on μ_4 and N is clear in both the experimental data and equation (11). Overall, $\langle H_{\max}/H_{1/3}\rangle$ of the experimental data is smaller than the MER H_{max} distribution; nevertheless, theoretical and experimental data show similar trends.

[21] Finally, Figure 10 shows the comparison between the experimental data and theory of freak wave occurrence frequency, P_{freak}. For small kurtosis waves, $\mu_4 < 3.5$, the freak wave occurrence frequency estimated by the MER $H_{\max}$ distribution is larger than what is obtained from the experimental data. This tendency is similar to Figure 6. However, the experimental data show a rapid growth of the occurrence probability of freak waves for larger kurtosis, $\mu_4 > 3.5$.

5. Conclusion

[22] Four wave quasi-resonant interactions play an important role in the determination of the statistical properties of the surface elevation. This discovery, which is fairly new, is of some relevance in the community of extreme wave forecasting. Previously, deviations from Gaussian behavior have been attributed only to bound modes. However, even for the most severe sea state conditions, the value of the kurtosis from second-order theory barely reaches values larger than 3.15. Moreover, the contribution to wave height distribution from second-order theory is practically negligible (in the narrow-band approximation it is exactly zero). If waves are long crested and sufficiently steep, the dynamics of the free waves can bring very strong departures from Gaussian expectation. In the experimental data analyzed in the present paper, values as high as 4.1 have been measured. Large values of kurtosis can substantially change the tails of the probability density function of wave height.

[23] In the present paper a detailed comparison between experimental data, consisting of a large number of waves, and the theoretical expectation described by *Mori and Janssen* [2006] have been discussed. The spatial evolution of kurtosis along the tank can be estimated by the quasi-resonant four wave interactions theory originally developed by *Janssen* [2003]. As the kurtosis increases, the probability of large amplitude waves also increases. The MER distribution is capable of describing with some accuracy the tail of the exceedance probability of wave heights for large kurtosis, i.e., for strong nonlinearity. Comparison of the MER distribution for maximum wave height with experimental data has also shown a much better agreement than when the maximum wave height distribution obtained from Rayleigh distribution is used. Overall, the theory originally described by Edgeworth at the beginning of the last century, combined with four wave quasi-resonant interaction theory and wave statistical theory seems to be an interesting approach for predicting extreme waves in long-crested conditions. We should emphasize here that the theory does not need any empirical, ad hoc parameter.

[24] In real sea states directional effects are important. In this paper we have concentrated on the idea of extreme wave generation owing to four wave interactions in a unidirectional wave train. Presently we are extending the theory to including directional wave effects. This will be discussed in near future.

[25] **Acknowledgments.** NM and MO wish to thank the European Centre for Medium-Range Weather Forecasts FOR financial support during their stay as visiting scientists there. NM also wishes to thank JSPS for financial support. We thank the European Union (contract HPRI-CT-2001-00176) for making the experiments in Marintek possible. C. T. Stansberg and L. Cavaleri are also acknowledged for their valuable help during the experiments.

References

Annekov, S., and V. Shrira (2006), Role of non-resonant interactions in evolution of nonlinear random water wave fields, *J. Fluid Mech.*, *561*, 181–207.
Boccotti, P. (1989), On mechanics of irregular gravity waves, *Atti Accad. Naz. Lincei Mem.*, *19*, 11–170.
Edgeworth, F. (1907), On the representation of statistical frequency by a series, *J. R. Stat. Soc.*, *70*, 102–106.
Fedele, F., and F. Arena (2005), Weakly nonlinear statistics of high nonlinear random waves, *Phys. Fluids.*, *17*, 026601, doi:10.1063/1.1831311.
Fedele, F., and A. Tayfun (2006), Explaining freak waves by a stochastic theory of wave groups, paper presented at 25th International Conference on Offshore Mechanics and Arctic Engineering, Am. Soc. of Mech. Eng., Hamburg, Germany.

Goda, Y. (2000), *Random Seas and Design of Maritime Structures*, 2nd ed., World Sci., Hackensack, N. J.

Guedes Soares, C., Z. Cherneva, and E. Antão (2003), Characteristics of abnormal waves in North Sea storm sea states, *Appl. Ocean Res.*, *25*, 337–344.

Guedes Soares, C., Z. Cherneva, and E. M. Antã o (2004), Abnormal waves during Hurricane Camille, *J. Geophys. Res.*, *109*, C08008, doi:10.1029/2003JC002244.

Hasselmann, K. (1962), On the nonlinear energy transfer in gravity-wave spectrum. I. Gerenral theory, *Jo. Fluid Mech.*, *12*, 481–500.

Janssen, P. (2003), Nonlinear four-wave interactions and freak waves, *J. Phys. Oceanogr.*, *33*, 863–884.

Krasitskii, V. (1994), On reduced equations in the Hamiltonian theory of weakly nonlinear surface waves, *J. Fluid Mech.*, *272*, 1–20.

Longuet-Higgins, M. (1952), On the statistical distribution of the heights of sea waves, *J. Mar. Res.*, *11*, 245–266.

Longuet-Higgins, M. (1963), The effect of non-linearities on statistical distributions in the theory of sea waves, *J. Fluid Mech.*, *17*, 459–480.

Marthinsen, T., and S. Winterstein (1992), On the skewness of random surface waves, in *Proceedings of the 2nd International Offshore and Polar Engineering Conference*, vol. 3, pp. 472–478, Int. Soc. of Offshore and Polar Eng., San Francisco, Calif.

Mori, N., and P. Janssen (2006), On kurtosis and occurrence probability of freak waves, *J. Phys. Oceanogr.*, *36*, 1471–1483.

Mori, N., and T. Yasuda (2002), A weakly non-Gaussian model of wave height distribution for random wave train, *Ocean Eng.*, *29*, 1219–1231.

Mori, N., T. Yasuda, and K. Kawaguchi (1997), Breaking effects on waves statistics for deep-water random wave train, in *Ocean Wave Measurement and Analysis (1997)*, edited by B. L. Edge and J. M. Hemsley, pp. 316–328, Am. Soc. of Civ. Eng., Reston, Va.

Mori, N., P. Liu, and T. Yasuda (2002), Analysis of freak wave measurements in the Sea of Japan, *Ocean Eng.*, *29*, 1399–1414.

Muller, P., and D. Henderson (Eds.) (2005), *Proceedings of Rogue Waves, Hawaiian Winter Workshop*, Univ. of Hawai'i at Manoa, Honolulu.

Næss, A. (1985), On the distribution of crest-to-trough wave heights, *Ocean Eng.*, *12*, 221–234.

Olagnon, M., , and M. Prevosto (Eds.) (2004), *Proceedings of Rogue Waves 2004*, Inst. Fr. de Rech. Pour l'Exploit. de la Mer, Brest.

Onorato, M., A. Osborne, M. Serio, and S. Bertone (2001), Freak waves in random oceanic sea states, *Phys. Rev. Lett.*, *86*, 5831–5834.

Onorato, M., A. Osborne, and M. Serio (2002), Extreme wave events in directional, random oceanic sea states, *Phys. Fluids*, *14*, L25–L28.

Onorato, M., A. Osborne, M. Serio, M. Brandini, and C. Stansberg (2004), Observation of strongly non-Gaussian statistics for random sea surface gravity waves in wave flume experiments, *Phys. Rev. E*, *70*, 067302, doi:10.1103/PhysRevE.70.067302.

Onorato, M., A. Osborne, and M.Serio (2005a), On deviations from Guassian statistics for surface gravity waves, in *Proceedings Rogue Waves, Hawaiian Winter Workshop*, edited by P. Muller and D. Henderson, pp. 79–83, Univ. of Hawai'i at Manoa, Honolulu.

Onorato, M., A. Osborne, M. Serio, and L. Cavaleri (2005b), Modulational instability and non-Gaussian statistics in experimental random water-wave trains, *Phys. Fluids*, *17*, 078101, doi:10.1063/1.1946769.

Onorato, M., A. Osborne, M. Serio, L. Cavaleri, C. Brandini, and C. Stansberg (2006), Extreme waves, modulational instability and second order theory: Wave flume experiments on irregular waves, *Eur. J. Mech. B*, *25*, 586–601.

Pelinovsky, E., and C. Kharif (2006), Rogue waves Vienna, Austria, *Eur. J. Mech. B*, *25*, 535–692.

Socquet-Juglard, H., K. Dysthe, K. Trulsen, H. E. Krogstad, and J. Liu (2005), Distribution of surface gravity waves during spectral changes, *J. Fluid Mech.*, *542*, 195–216.

Stansell, P., J. Wolfram, and S. Zachary (2003), Horizontal asymmetry and steepness distributions for wind-driven ocean waves, *Appl. Ocean Res.*, *25*, 137–155.

Tayfun, M. (1980), Narrow band nonlinear sea waves, *J. Geophys. Res.*, *85*, 1548–1552.

Tayfun, M. (1981), Distribution of crest-to-trough wave heights, *J. Waterw. Port Coastal Ocean Eng.*, *107*, 149–158.

Tayfun, M. (2006), Statistics of nonlinear wave crests and groups, *Ocean Eng.*, *33*, 589–1622.

Tayfun, M., and J.-M. Lo (1990), Nonlinear effects on wave envelope and phase, *J. Waterw. Port Coastal Ocean Eng.*, *116*, 79–100.

Yasuda, T., and N. Mori (1994), High order nonlinear effects on deep-water random wave trains, in *Waves—Physical and Numerical Modelling*, vol. 2, edited by M. Isaacson and M. C. Quick, pp. 823–332, Vancouver, B. C., Canada.

Yasuda, T., and N. Mori (1997), Occurrence properties of giant freak waves the sea area around Japan, *J. Waterw. Port Coastal Ocean Eng.*, *123*, 209–213.

Yasuda, T., N. Mori, and K. Ito (1992), Freak waves in a unidirectional wave train and their kinematics, in *Coastal Engineering (1992)*, vol. 1, edited by B. L. Edge, pp. 751–764, Am. Soc. of Civ. Eng., Reston, Va.

Yasuda, T., N. Mori, and S. Nakayama (1997), Characteristics of giant freak waves observed in the Sea of Japan, in *Ocean Wave Measurement and Analysis (1997)*, edited by B. L. Edge and J. M. Hemsley, pp. 482–495, Am. Soc. of Civ. Eng., Reston, Va.

P. A. E. M. Janssen, European Centre for Medium-Range Weather Forecasts, Shinfield Park, Reading RG2 9AX, UK. (peter.janssen@ecmwf.int)

N. Mori, Graduate School of Engineering, Osaka City University, Osaka 558-8585, Japan. (mori@urban.eng.osaka-cu.ac.jp)

M. Onorato, A. R. Osborne, and M. Serio, Dipartmento di Fisica Generale, Università di Torino, Via P. Giardia, I-10125 1-Torino, Italy. (onorato@ph.unito.it; osborne@to.infn.it; marina.serio@unito.it)